

INSTITUTE FOR FUSION STUDIES

DOE/ET-53088-485

IFSR #485

Analysis of Tokamak Plasma Vertical Stability
by Rigid-Displacement and
Resistive-MHD Methods

R.R. KHAYRUTDINOV, E.A. AZIZOV,¹ R. CARRERA,² J.Q. DONG,³
and E. MONTALVO²

Institute for Fusion Studies
The University of Texas at Austin
Austin, Texas 78712

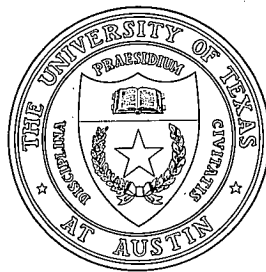
April 1991

¹I.V. Kurchatov Institute of Atomic Energy, Moscow, USSR

²Center for Fusion Engineering, UT-Austin, Austin, Texas

³Southwestern Institute of Physics, Leshan, China

THE UNIVERSITY OF TEXAS



AUSTIN

Analysis of Tokamak Plasma Vertical Stability
by Rigid-Displacement
and Resistive-MHD Methods

R. R. Khayrutdinov, E. A. Azizov¹, R. Carrera², J. Q. Dong³, E. Montalvo²

Institute for Fusion Studies
The University of Texas at Austin
Austin, Texas 78712

Stability and control of the vertical position of tokamak plasmas are studied using the "rigid displacement" and the resistive MHD models. In the rigid displacement model the plasma current and plasma shape are assumed not to change with time. The plasma, the vacuum vessel, and the active conductors are represented by a set of rigid, axisymmetric filaments. In the resistive MHD model no limitations on the time variation of the plasma shape and current are imposed. The circuit equations for the eddy currents in the vacuum vessel and the passive coils, and the currents induced in active conductors are solved simultaneously with the equilibrium and transport equations for the plasma. The plasma response to a step-control signal is studied. A detailed comparison between the two simulation methods is presented. It is shown that the resistive MHD model predicts a more stable plasma than the rigid displacement model. The computational time advantage of the rigid displacement analysis over conventional resistive MHD calculations is almost outweighed by the numerical algorithm used in the integration scheme of the DINA code employed here.

¹ Permanent address: I.V. Kurchatov Institute of Atomic Energy, Moscow, USSR

² Center for Fusion Engineering, The University of Texas at Austin.

³ Southwestern Institute of Physics, Leshan, China.

Introduction

It is well known that elongated tokamak plasmas are generally unstable to an axisymmetric vertical displacement. The vacuum vessel and passive conductors usually stabilize the fast plasma motion. For stabilization of slow plasma motions, an active feedback control system is required. For the definition of a feedback system, a detailed simulation of the characteristics and operation of the active control system is required. In this paper, the plasma response to a step-control signal, and its voltage and current trajectories are studied. We determine the characteristics of the active control system such as gain, lead time, delay time, and power supply specifications.

We consider two approaches for the investigation of this problem. In the first method, the plasma consists of a set of rigid, current filaments. It is assumed that no changes in current and plasma shape are produced throughout the plasma motion. This model is named the “rigid displacement” (RD) model. In the second (the most exact), no limitations on the plasma shape and current time variation are imposed. The circuit equations for the eddy currents in the vacuum vessel and the currents in the active conductors are solved simultaneously with the equilibrium and transport equations for the plasma. The plasma current and shape change during the plasma motion when a control input signal is applied to the active control coils.

The purpose of this work is to study tokamak vertical stability and control using these two approaches. We want to find the regions of the stability diagram where both methods give similar results and the regions where there are discrepancies. The numerical simulation has been carried out for the IGNITEX configuration [1-4]. The code DINA [5] is used in the second approach. In this method the evolution of the plasma with free boundary in externally changing magnetic fields is modelled. The problem is coupled with the currents in the vacuum vessel, passive, and active coils. The plasma current filaments for the RD model are defined from the solution of the resistive MHD (RMHD) equilibrium problem (at the midplane plasma position).

Rigid displacement model

An axisymmetric vertical plasma displacement in a tokamak configuration can be

described by a system of equations which includes: force balance, circuit equation, and voltage control law. The plasma is modelled by a set of rigid, current filaments. The coordinates and the currents of the plasma filaments are determined from the result of a plasma equilibrium calculation. The vacuum vessel and the poloidal field coils are represented by a set of filaments. The equation for plasma motion in the RD approximation can be written as:

$$m\ddot{z} = - \sum_{i=1}^{N_p} \frac{\partial B_{ri}}{\partial z} \frac{2\pi R_i}{c} I_{pi} z - \sum_{j=1}^M \sum_{i=1}^{N_p} B_{ij} I_{pi} \frac{2\pi R_i}{c} I_j$$

where m is the plasma mass; N_p is the number of plasma filaments; c is the speed of light; R_i is the major radius of the i^{th} plasma filament; B_{ri} is the external radial magnetic field on the i^{th} plasma filament; B_{ij} is the radial magnetic field produced by the induced and the active-coil unit currents on the i^{th} plasma filament; I_{pi} and I_j are the currents in the plasma and the external filaments, respectively; M is the total number of non-plasma filaments including those in the vacuum vessel, the poloidal field coils, the passive coils, and the active coils; z is the plasma displacement; and \ddot{z} is the acceleration of the plasma column. We use the following notation:

$$S_b = - \sum_{i=1}^{N_p} \frac{\partial B_{ri}}{\partial z} \frac{2\pi R_i}{c} I_{pi},$$

$$S_j = - \sum_{i=1}^{N_p} B_{ij} I_{pi} \frac{2\pi R_i}{c}, \quad \text{and}$$

$$S_j^M = \sum_{i=1}^{N_p} I_{pi} \frac{\partial M_{ij}}{\partial z}.$$

Thus, the plasma equation of motion and the circuit equations can be written as:

$$m\ddot{z} = S_b z + \sum_{j=1}^M S_j I_j, \quad \text{and}$$

$$L_j \dot{I}_j + \sum_{k \neq j}^M M_{jk} \dot{I}_k + \tilde{R}_j I_j + S_j^M \dot{z} = V_j,$$

where M_{jk} is the mutual inductance between the k^{th} and j^{th} filaments; \tilde{R}_j is the resistance of j^{th} filament; M_{ij} is the mutual inductance between the j^{th} filament and i^{th} plasma filament; and V_j is the voltage imposed on the j^{th} filament.

The stability of the system is determined by the character of the voltage applied to the feedback control coils. A general control law is considered here. The equation contains proportional terms, derivative terms, and various time constants for the feedback control system. The control law is written as:

$$t_b t_c \ddot{V}_j + (t_b + t_c) \dot{V}_j + V_j = -g_j \{ (z - z_{ref}) + t_a (\dot{z} - \dot{z}_{ref}) \},$$

where g_j is the gain on the j^{th} active control coil; z_{ref} is the reference plasma position; t_b is the delay time of the active control system; and, t_a and t_c are the lead and lag (filter) system time constants, respectively.

The full system of equations can be expressed in matrix form as:

$$\hat{B} \dot{\vec{x}} = \hat{A} \vec{x} + \vec{F}, \quad (1)$$

where $\vec{x} = \{z, \dot{z}, I_j, V_k, \dot{V}_k\}$; $j = 1, \dots, M$; $k = 1, \dots, N_{ac}$;

$\vec{F} = \{0, \dots, g_k(z_{ref} + t_a \dot{z}_{ref}, \dots, 0\}$, $k = 1, \dots, N_{ac}$; N_{ac} is the number of active-coil filaments. First we consider the homogeneous system

$$\hat{B} \dot{\vec{x}} = \hat{A} \vec{x}. \quad (2)$$

The Laplace transform of Eq.(2) is:

$$\lambda B \vec{x} = A \vec{x}.$$

Denoting by λ_j the j^{th} eigenvalue and by \vec{u}_j the j^{th} eigenvector, the general solution of the system can be written as

$$\vec{x}(t) = \sum_k a_k \vec{u}_k e^{\lambda_k t}, \quad (3)$$

where the a_k 's are general constant coefficients. In solving Eq.(1) we assume that the coefficients a_k are time dependent, i.e, $a_k = a_k(t)$. Substituting Eq.(3) in Eq.(1) we obtain

$$\hat{B} \left(\sum_k \dot{a}_k \vec{u}_k e^{\lambda_k t} \right) = \vec{F}. \quad (4)$$

Using $\varphi_k = \dot{a}_k e^{\lambda_k t}$, then Eq.(4) can be rewritten as:

$$\hat{B} \left(\sum_k \varphi_k \vec{u}_k \right) = \vec{F},$$

or

$$\sum_k \varphi_k (\hat{B} \vec{u}_k) = \vec{F}.$$

Let $\vec{d}_k = \hat{B} \vec{u}_k$, then $\sum_k \varphi_k \vec{d}_k = \vec{F}$ or $\sum_k d_{ik} \varphi_k = F_i$, which is equivalent to

$$\hat{d} \vec{\varphi} = \vec{F}. \quad (5)$$

Solving the matrix equation (5) we obtain vector $\vec{\varphi}$. After integration, we obtain

$$a_k(t) = -\frac{\varphi_k}{\lambda_k} e^{-\lambda_k \tau} \Big|_0^t + a_k(0). \quad (6)$$

Substituting in Eq.(3) we obtain the solution

$$\vec{x}(t) = \sum_k a_k(t) e^{\lambda_k t} \vec{u}_k = \left\{ -\frac{\varphi_k}{\lambda_k} (1 - e^{\lambda_k t}) + a_k(0) e^{\lambda_k t} \right\} \vec{u}_k. \quad (7)$$

Eq.(7) describes the time response of the plasma to a control-input signal when the eigenvalues λ_k , the eigenvectors \vec{u}_k , and the initial conditions $\vec{x}(0)$ are known. If $z_{ref} = 0$, then $\vec{F} = 0$, and the coefficients $\{a_k\}$ are constants. The coefficients $\{a_k\}$ are determined by the initial conditions from:

$$\vec{x}(0) = \sum_k a_k \vec{u}_k. \quad (8)$$

The quantities λ_j and \vec{u}_j are usually complex. For plasma stability it is necessary that the real parts of all eigenvalues be negative.

Resistive MHD model

The evolution of a free boundary tokamak plasma in an external, changing magnetic field is modelled using the code DINA [5]. The equilibrium problem in 2-D geometry coupled with the system of 1-D transport equations (obtained by averaging on magnetic surfaces) is solved. The eddy currents induced in the vacuum vessel and in the poloidal field coils are evaluated. The plasma parameters (current, temperature, density, poloidal flux, toroidal flux, and so on) are obtained. The vacuum vessel and the passive and active control coils are described by circuit equations of the form:

$$L_j \dot{I}_j + \sum_{k \neq j}^M M_{jk} \dot{I}_k + \bar{R}_j I_j + \dot{\Psi}_p^j = V_j, \quad (9)$$

where $\dot{\Psi}_p^j$ is the poloidal flux produced by the plasma on the j^{th} filament. The control voltage applied to the active coils has the form

$$t_b \dot{V}_j + V_j = -g_j \{ (z - z_{ref}) + t_a (\dot{z} - \dot{z}_{ref}) \},$$

where $t_c = 0$ is considered here.

Stability analysis

The poloidal field configuration and the position of the active coils used here are shown in Fig.1. We study the plasma behaviour and the active control system using a control-step input with a proportional law for the voltage applied to the active coils. This voltage has the form $V = -g(z - z_{ref})$, where $z_{ref} = 1 \text{ cm}$. For various gain values we calculate the plasma time responses and thus, find the values of gain required for plasma stability. These values lie in a region $g_{min} < g < g_{max}$, where g_{min} is the minimum gain which stabilizes the plasma and g_{max} is maximum gain for plasma stability. For $g > g_{max}$, the plasma oscillates and becomes unstable.

When we compare the values g_{min} and g_{max} obtained using the two models described before, we find some differences. The values of g_{min} in the RD and RMHD models are rather similar. The value of g_{max} is higher in the RMHD calculation than in the RD calculation. The regions of the stability for both models are shown in Fig.2.

The plasma time response to a step-input voltage when a plasma reference position (z_{ref}) is imposed is shown in Fig.3. Here the plasma displacement is given as a function of time. With low gain we obtain a large steady state error in the plasma position. In Fig.3-a for a gain $g = 550 V/m$ the plasma becomes stable in both models. In Fig.3-b for a gain $g = 3 \cdot 10^5 V/m$, the plasma becomes unstable with RD but is stable with RMHD. In Fig.3-c for $g = 7 \cdot 10^5 V/m$, the plasma is unstable in both cases. Higher gain values lead to decreasing steady state errors.

The time responses for the two models are shown in Fig. 4 (for $g = 1000 V/m$ and $g = 4500 V/m$). For $g = 4500 V/m$, the steady state error is small.

It is interesting to compare the results using a more complicated voltage law:

$$t_b \dot{V} + V = -g \{ (z - z_{ref}) + t_a (\dot{z} - \dot{z}_{ref}) \} ,$$

for various values of t_b , t_a , and g . The results of the analysis for $t_b = 10 ms$, $t_a = 0$; $t_b = 0$, $t_a = 10 ms$; and $t_b = 10 ms$, $t_a = 10 ms$ are given in Figs.5-a, 5-b, 5-c, respectively. It is seen that with RD, the plasma oscillates more than in the RMHD analysis. However the values of current and voltage required for control in the active coils are very similar in both models. For $t_a = 0$, $t_b = 10 ms$, and $g = 4500 V/m$ the plasma becomes unstable with both models.

We have considered the limiting case when plasma is represented as a single filament located at the magnetic axis. For the case of pure proportional gain with $g = 4500 V/m$ the plasma is unstable. Adding in the voltage control law a derivative term with $t_a = 10 ms$ stabilizes the plasma (plasma displacements for these cases are illustrated in Fig.6).

A detailed stability analysis has been carried out for the case of small gain $g = 450 V/m$. Here the plasma is unstable and oscillates several times before hitting the vacuum vessel. Fig.7 gives the plasma magnetic surfaces at times $t_1 = 400ms$ and $t_2 = 700ms$, respectively. In Figs.8 - a, b we show the time dependence of the plasma current and the safety factor (at the boundary) during the oscillations. In Fig.8 - c we give the current density profile at various times throughout the simulation. It is seen that, when the plasma shape changes, the safety factor at the boundary also changes, but the total plasma current changes only slightly. The plasma current remains rather constant because

of the low plasma resistivity. Skin effects are observed when the plasma is changing shape.

Conclusions

It has been shown numerically that in the RMHD model analysis the stable region is wider than in RD model analysis. Comparing plasma motions with the same gain, it is seen that the plasma oscillates in the RD analysis more than in the RMHD analysis. In the case when plasma is represented as a single filament the system becomes unstable for values of gain within the stable region (for both the RD and the RMHD methods). The dependence of the plasma response on the time constants t_a and t_b in RD is similar to that in RMHD. Since the simulations with RD are somewhat faster than with RMHD, RD simulations should be used to obtain preliminary evaluations of stability diagrams and positioning of active control coils. These preliminary estimates can be used as a first estimate for the RMHD simulation. Our RMHD approach permits to obtain accurate estimates of the plasma response. Although our RMHD approach is more time consuming than RD approach still is much faster than the conventional methods [6].

References

1. R. Carrera and E. Montalvo, "Fusion Ignition Experiment", *Nuclear Fusion*, **30**, 891, (1990).
2. M. N. Rosenbluth, W. F. Weldon, and H. H. Woodson, "Basic Design Report for the fusion Ignition Experiment (IGNITEX)", Center for Fusion Engineering Report, The University of Texas at Austin (March, 1987).
3. IGNITEX Group, "Description of the Scientific and Technological Aspects of the Fusion Ignition Experiment IGNITEX, " Ninth Topical Meeting on the Technology of Fusion Energy, Oak Brook, Illinois (October, 1990); *FusionTecnology*, **18**, 00 (1991).
4. R. R. Khayrutdinov, J. Q. Dong, E. Montalvo, E. A. Azizov, R. Carrera, W. D. Booth, and M. N. Rosenbluth, "Discharge Control in an Ignition Single-Turn-Coil Tokamak", Ninth Topical Meeting on the Technology of Fusion Energy, Oak Brook, Illinois (October, 1990); *Fusion Technology* **18**, 00 (1991).
5. R. R. Khayrutdinov, V. E. Lukash, "Studies of Plasma Equilibrium and Transport in a Tokamak Fusion Device with the Inverse-Variable Technique", Institute for Fusion Studies Report IFSR #471 January (1991), submitted to the *Journal of Computational Physics*.
6. S. C. Jardin, N. Pomphrey, and J. DeLucia, "Dynamic Modeling of Transport and Positional Control of Tokamaks", *Journal of Computational Physics*, **66**, 481 (1986).

Figure captions

Fig.1. Poloidal field coil system. Location of the active control coils.

Fig.2. Values of gains when plasma is stable:

- a) rigid displacement model
- b) resistive MHD model

Fig.3. Plasma response to control input signal with voltage control law $V = -g(z - z_{ref})$, where $z_{ref} = 1cm$ (a: resistive MHD, b: rigid displacement model).

- a) $g = 550 V/m$
- b) $g = 3 \times 10^4 V/m$
- c) $g = 7 \times 10^5 V/m$

Fig.4. Plasma response to control input signal with voltage control law $V = -g(z - z_{ref})$, where $z_{ref} = 1cm$ (a: resistive MHD, b: rigid displacement model).

- a) $g = 1000 V/m$
- b) $g = 4500 V/m$

Fig.5. Plasma response to control input signal with voltage control law $t_b \dot{V} + V = -g\{z - z_{ref} + t_a(\dot{z} - \dot{z}_{ref})\}$, where $z_{ref} = 1cm$ (a: resistive MHD, b: rigid displacement model).

- a) $g = 4500 V/m, t_b = 10 ms, t_a = 0$
- b) $g = 4500 V/m, t_a = 10 ms, t_b = 0$
- c) $g = 4500 V/m, t_a = 10 ms, t_b = 10 ms$

Fig.6. Plasma response to control input signal with voltage control law $t_b \dot{V} + V = -g\{z - z_{ref} + t_a(\dot{z} - \dot{z}_{ref})\}$, where $z_{ref} = 1cm$ (single plasma filament).

- a) $g = 4500 V/m, t_b = 0, t_a = 10 ms$
- b) $g = 4500 V/m, t_a = 0, t_b = 0$

Fig.7. Plasma magnetic surfaces at various times.

- a) $t = 400 ms, I_p = 10.9 MA$
- b) $t = 700 ms, I_p = 11.1 MA$

Fig.8. Time evolution of plasma characteristics:

A) plasma current, internal inductance, safety factor at boundary q_a and toroidal flux.

B) evolution of plasma current density at surface $z = 0$.

a) $t = 400 \text{ ms}$

b) $t = 550 \text{ ms}$

c) $t = 700 \text{ ms}$

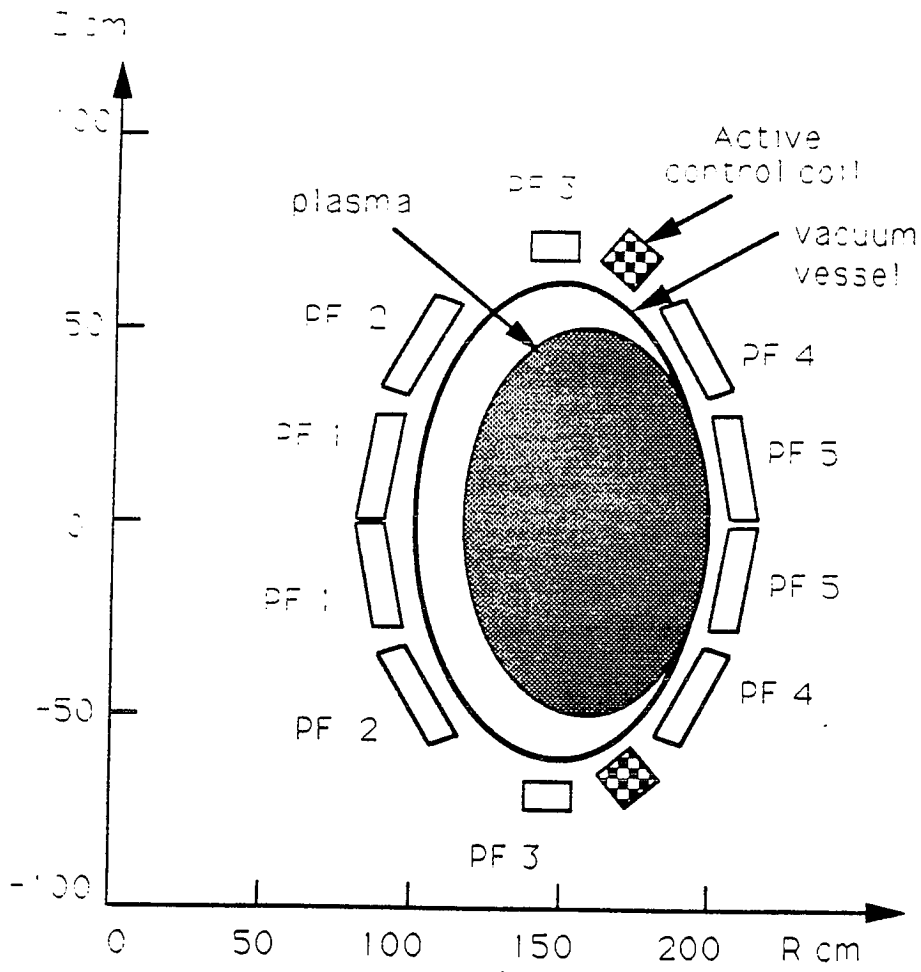


Fig.1

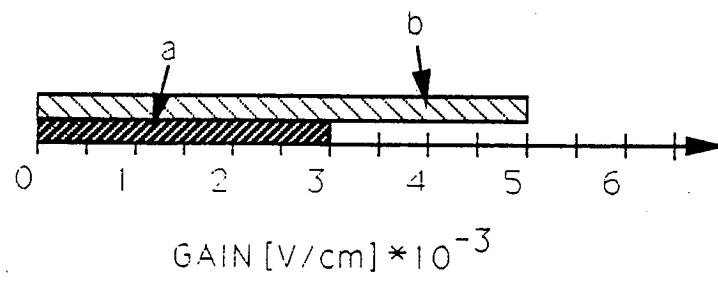


Fig.2

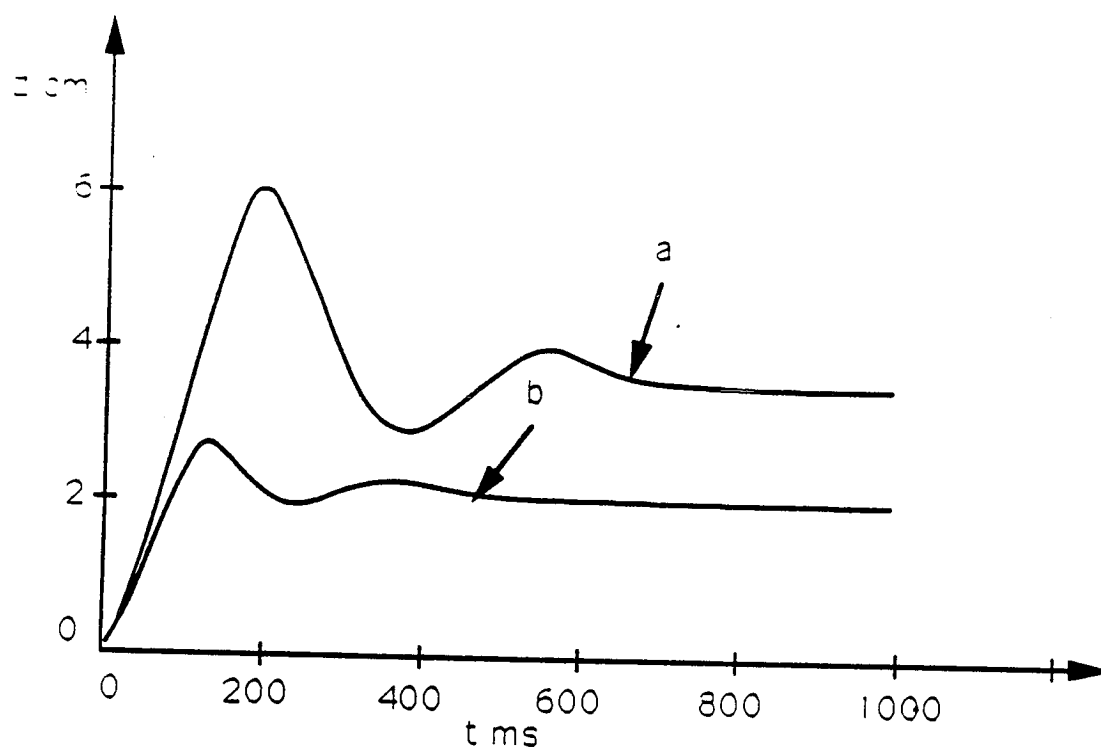


Fig.3-a

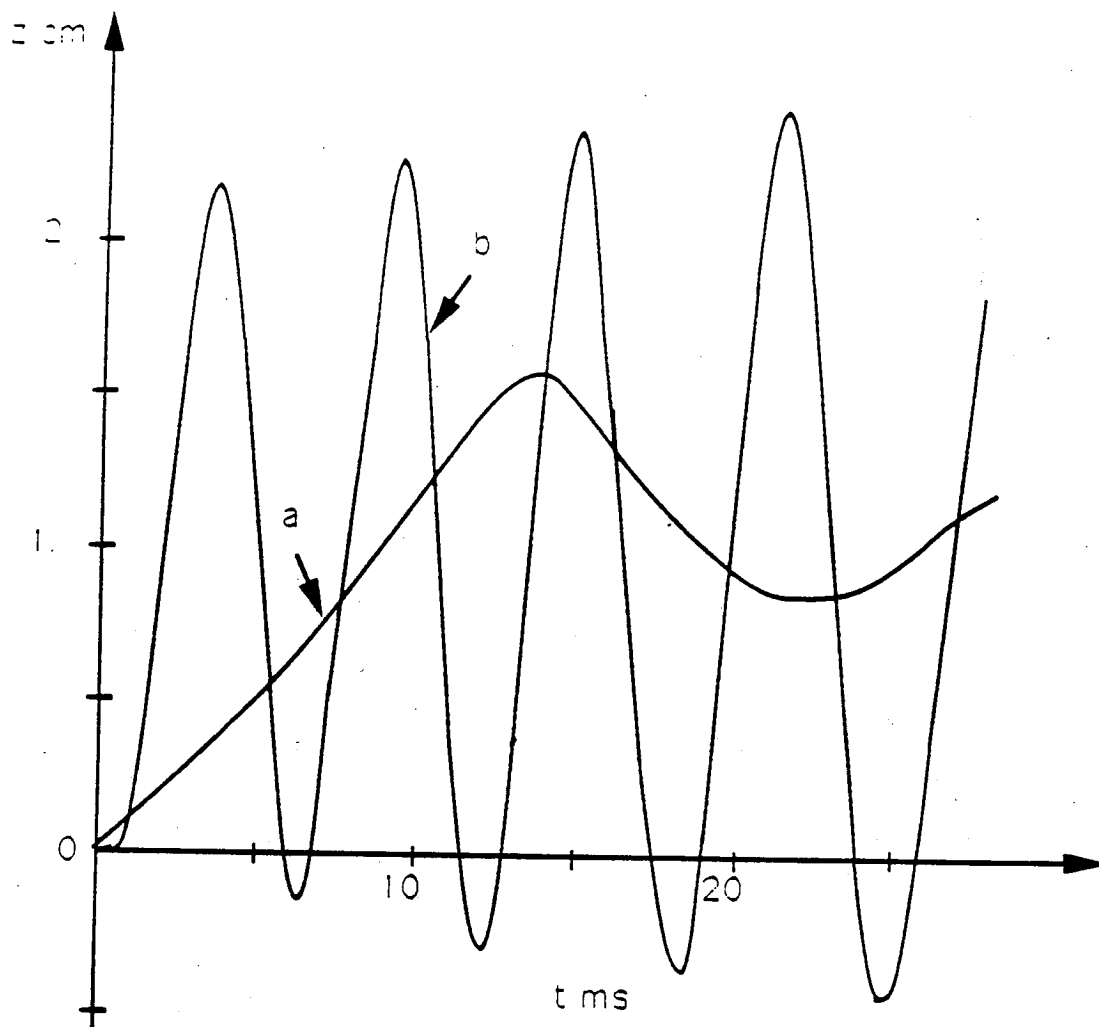


Fig.3-b

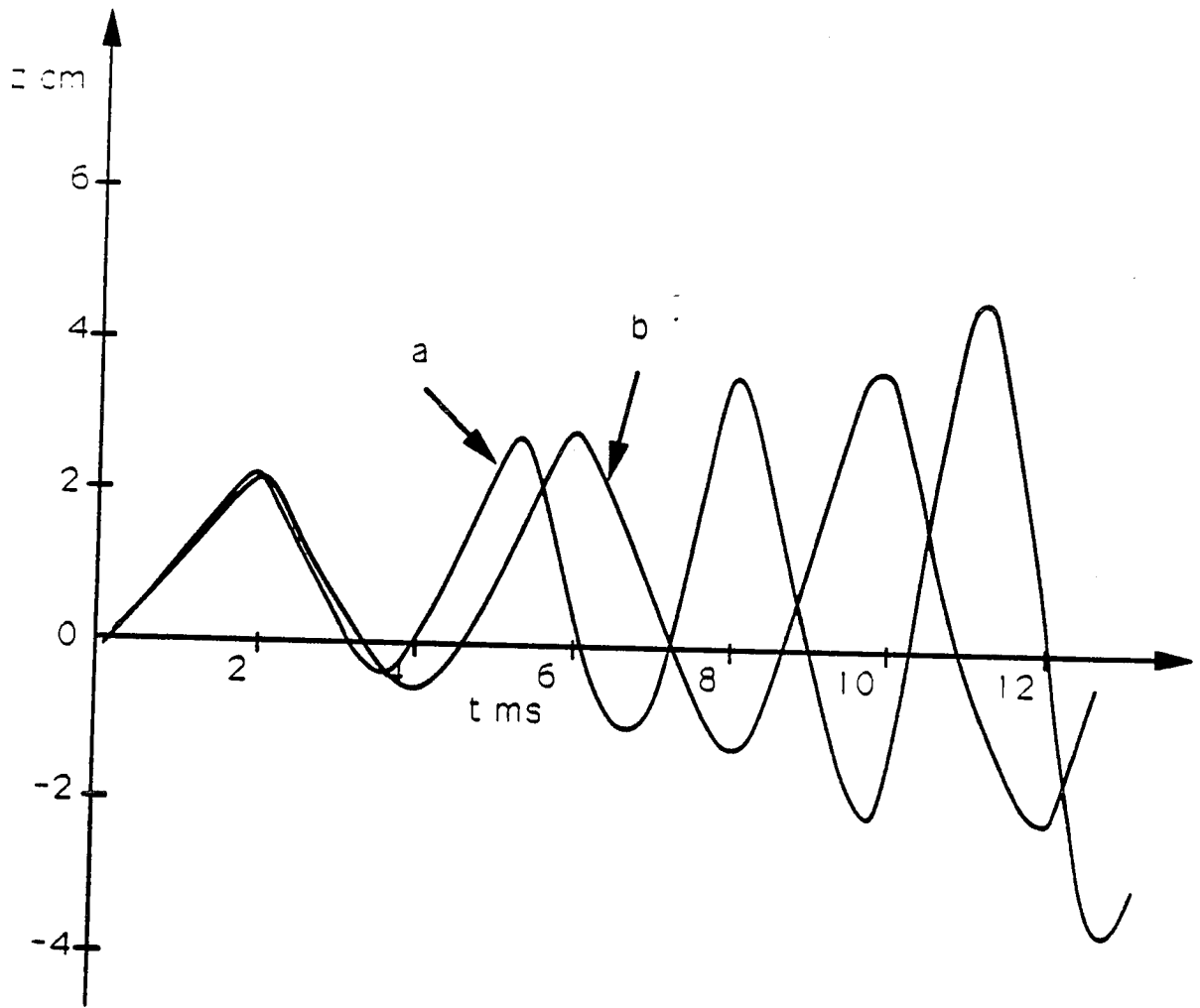


Fig.3-c

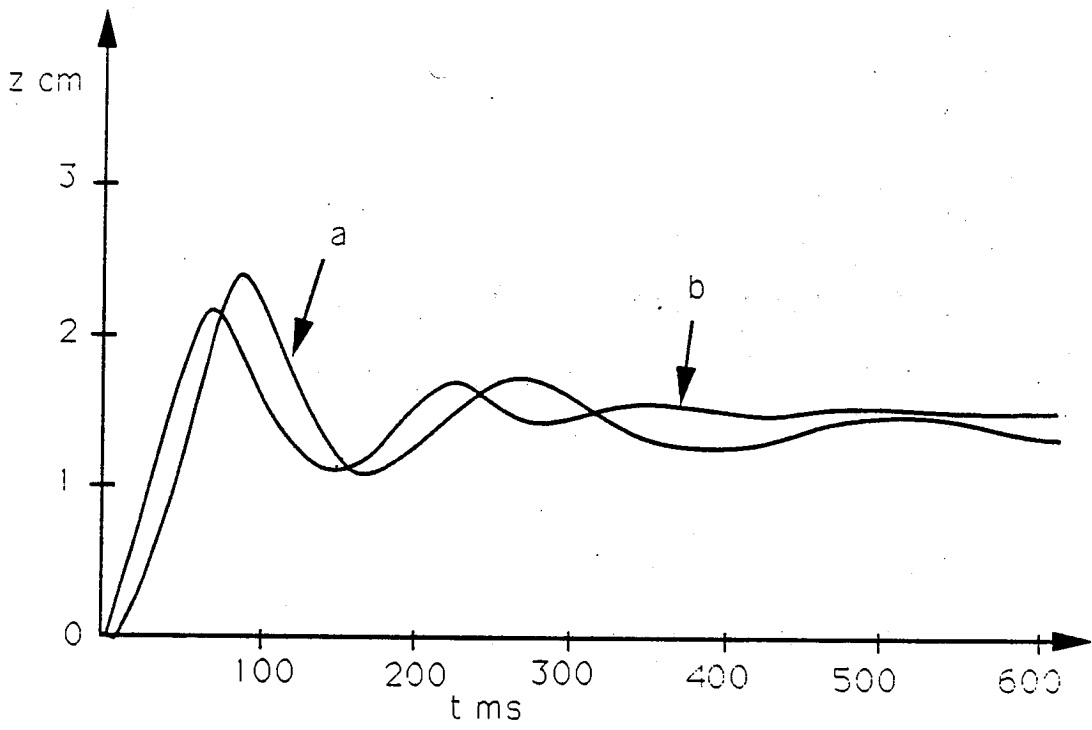


Fig.4-a

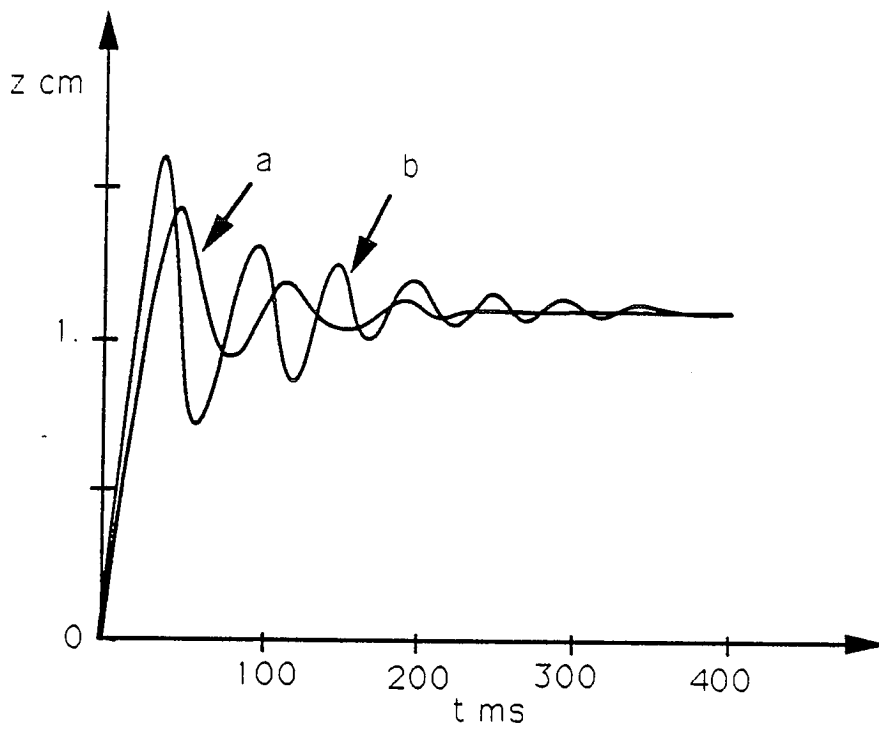


Fig.4-b

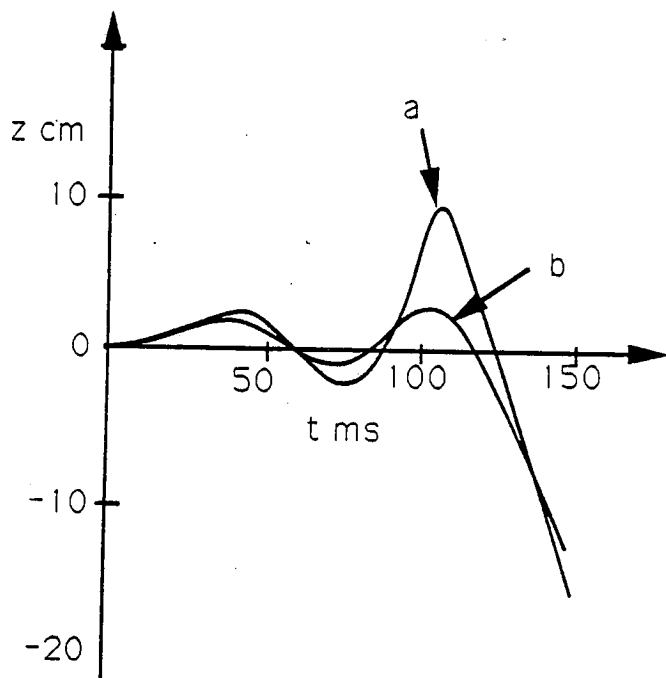


Fig.5-a

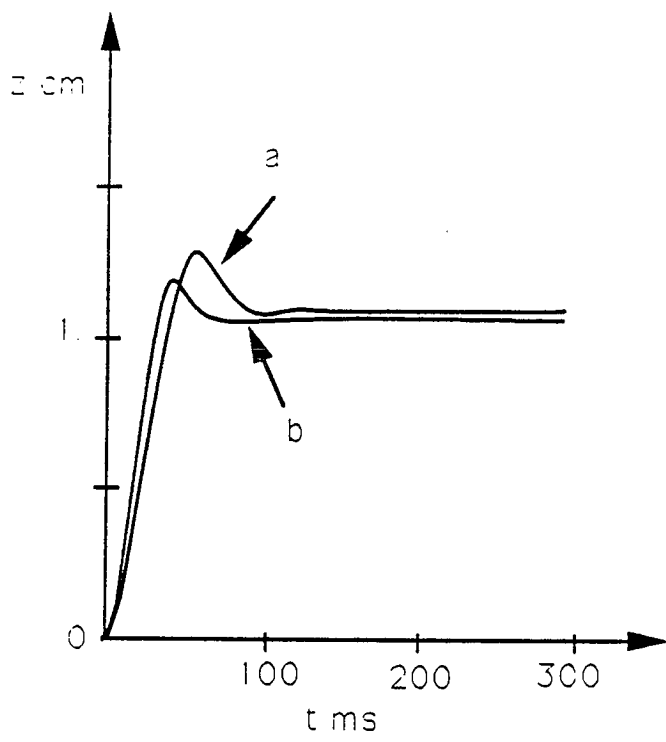


Fig.5-b

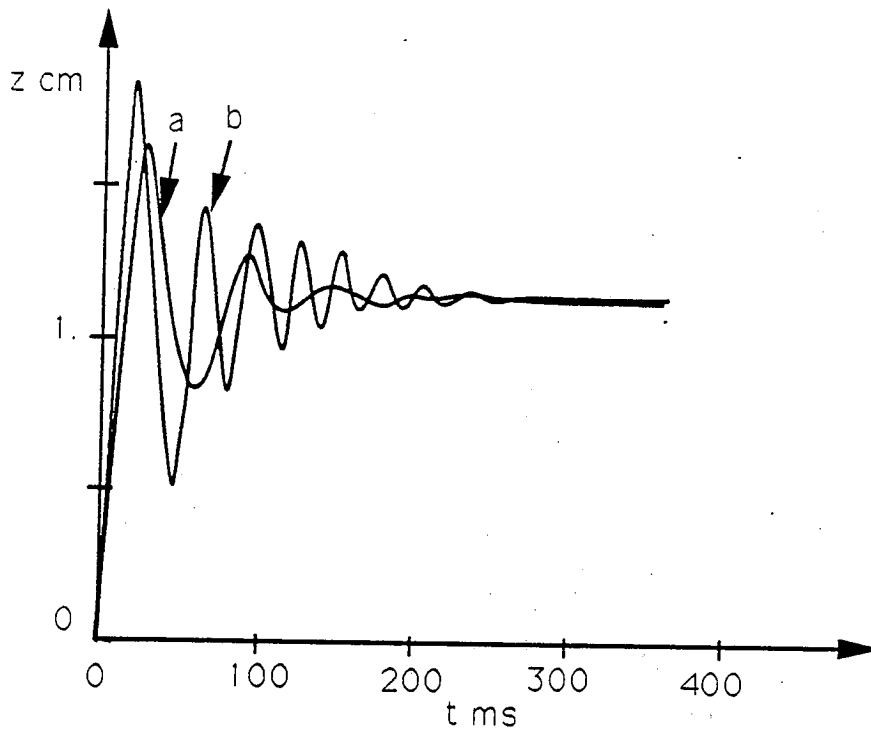


Fig.5-c

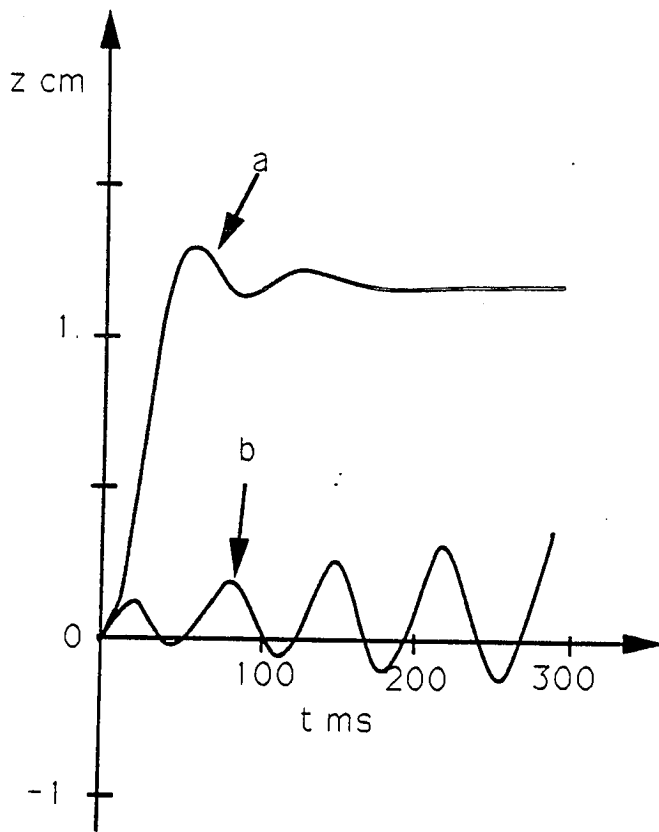


Fig.6

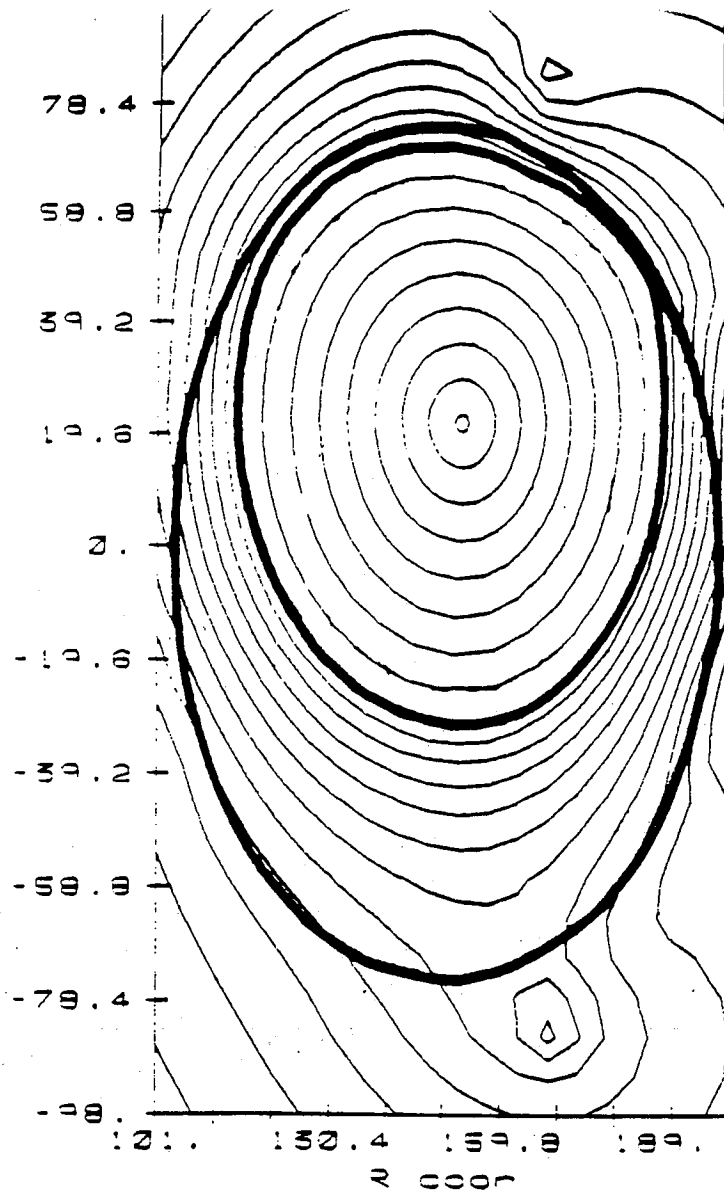


Fig.7-a

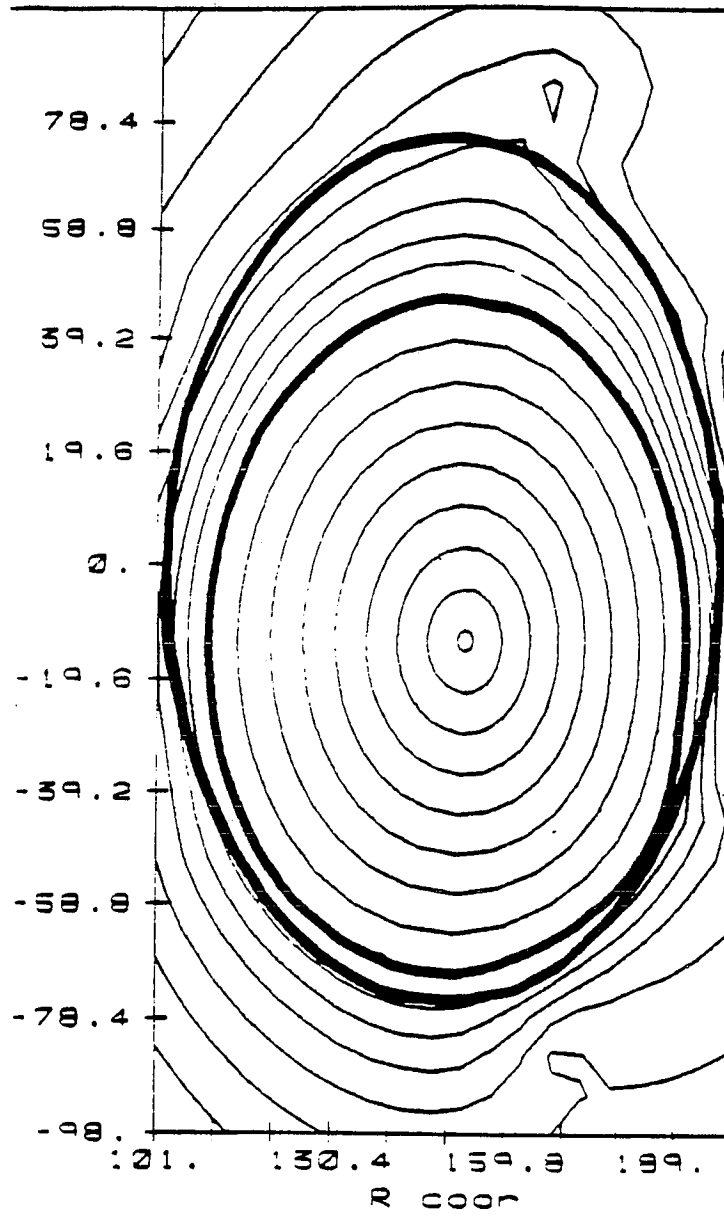


Fig.7-b

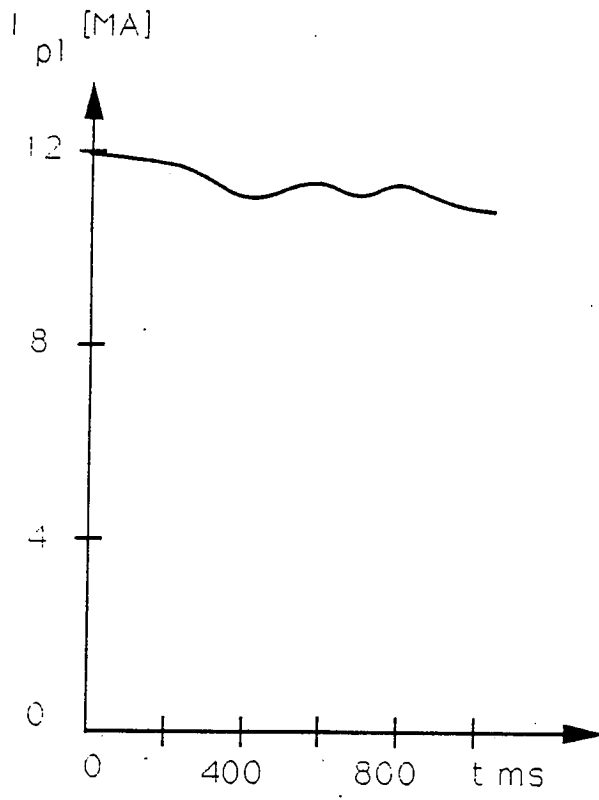


Fig.8-a

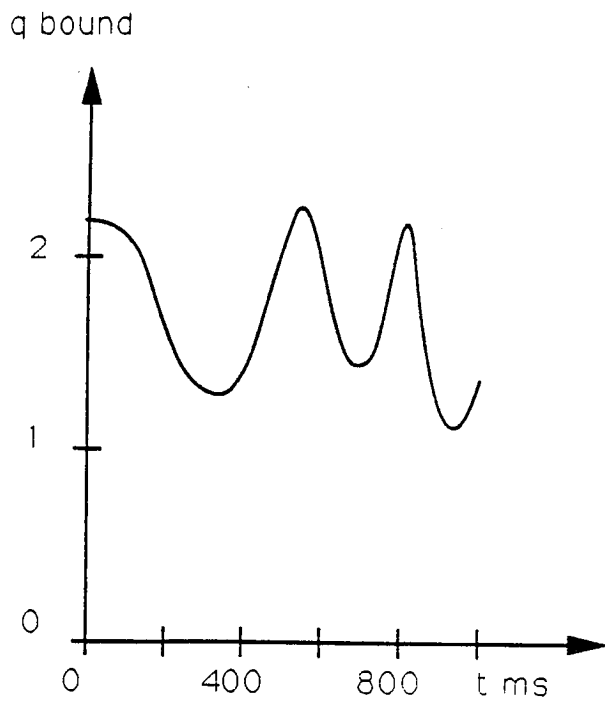


Fig.8-b

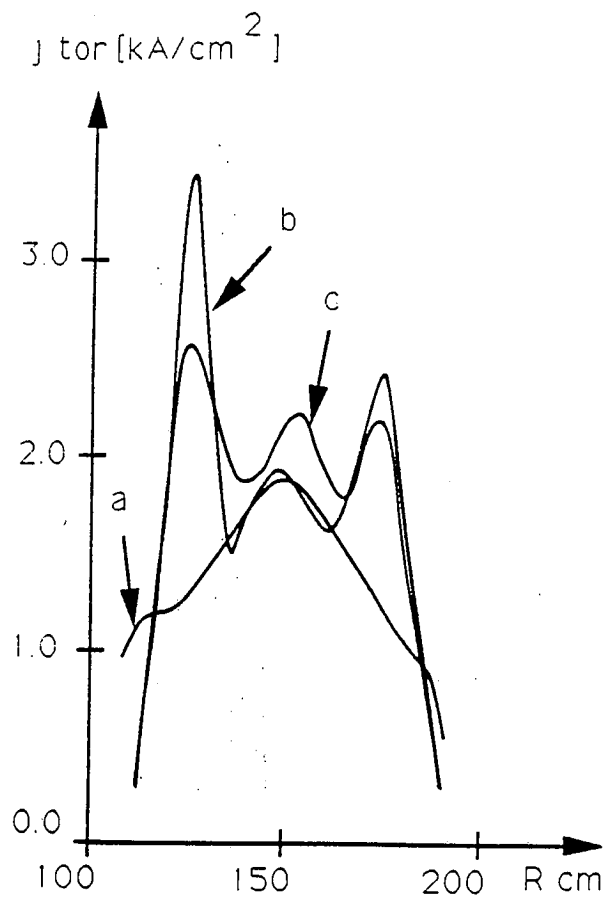


Fig.8-c

